DISPLACEMENT ANALYSIS OF NON-CIRCULAR PLANAR CURVED BEAMS UNDER IN-PLANE IMPULSIVE LOAD

A Thesis Submitted to
the Graduate School of Engineering and Sciences of
İzmir Institute of Technology
in Partial Fulfillment of the Requirements for the Degree of

MASTER OF SCIENCE

in Mechanical Engineering

by
Ahmet ÇELİK

October 2015
İZMİR

We approve the thesis of **Ahmet ÇELİK**

Examining Committee Members:

Prof. Dr. Bülent YARDIMOĞLU
Department of Mechanical Engineering, İzmir Institute of Technology

Assist. Prof. Dr. Onursal ÖNEN
Department of Mechanical Engineering, İzmir Institute of Technology

Assoc. Prof. Dr. Levent MALGACA
Department of Mechanical Engineering, Dokuz Eylül University

16 October 2015

Prof. Dr. Bülent YARDIMOĞLU
Supervisor, Department of Mechanical Engineering,
İzmir Institute of Technology

Prof. Dr. Metin TANOĞLU
Head of the Department of
Mechanical Engineering

Prof. Dr. R. Bilge KARAÇALI
Dean of the Graduate School
of Engineering and Sciences

ACKNOWLEDGEMENTS

Foremost, I would like to express my sincere gratitude to my advisor Prof. Bulent YARDIMOGLU for the continuous support of my M. Sc study and research, for his patience, motivation, enthusiasm, and immense knowledge. His guidance helped me in all the time of research and writing of this thesis. I could not have imagined having a better advisor and mentor for my M. Sc study.

ABSTRACT

DISPLACEMENT ANALYSIS OF NON-CIRCULAR PLANAR CURVED BEAMS UNDER IN-PLANE IMPULSIVE LOAD

In this study, time response of a planar curved beam with variable curvatures under in-plane impact load is analyzed by two numerical methods which are Finite Difference and Finite Element Methods. The solution procedures in both methods are based on solution of eigenvalue and time response problems. Catenary form is selected as the axis of curved beam. A computer program is developed in Mathematica for the solution with Finite Difference Method. Moreover, a computer code is written for the geometric and finite element models of curved beam with variable curvature in ANSYS by using APDL (ANSYS Parametric Design Language). Solutions of the two methods are compared in each other and then good agreement is observed. The effects of impuls and damping properties on the time response are investigated.

ÖZET

DÜZLEM İÇİ İMPULSİF KUVVET ALTINDAKİ DAİRESEL OLMAYAN DÜZLEMSEL EĞRİ ÇUBUKLARIN YERDEĞİŞTİRME ANALİZİ

Bu çalışmada, düzlem içi darbe yükü altındaki değişken eğrilikli düzlemsel eğri çubukların zaman cevabı sayılsal yöntemler olan Sonlu Farklar ve Sonlu Elemenlar Yöntemleri ile incelenmiştir. Her iki metoddaki çözüm usulü özdeğer ve zaman cevabı problemlerine dayalıdır. Eğri çubuğun ekseni olarak Katenary biçimi seçilmiştir. Sonlu Farklar Yöntemi ile çözüm için Mathematica'da bir program geliştirilmiştir. Ayrıca, değişken eğrilikli eğri çubuğun geometrik ve sonlu eleman modelleri için ANSYS de APDL (ANSYS Parametrik Tasarım Dili) ile bir bilgisayar kodu yazılmıştır. İki metodun çözümleri birbirleri ile karşılaştırılmış ve iyi bir uyum gözlenmiştir. İmpuls ve sönüm özelliklerinin zaman cavabına etkileri araştırılmıştır.

TABLE OF CONTENTS

LIST OF FIGURES

Figure **Page**

LIST OF TABLES

LIST OF SYMBOLS

A	cross-sectional area
b	width of the beam
B	bending stiffness
$C[\ ]$	differential operator for damping
[C]	damping matrix
E	modulus of elasticity
$f_0(s)$ - $f_6(s)$	variable coefficients of differential equation
f_i	i^{th} natural frequency
F_n	external force in normal direction
F_t	external force in tangential direction
$F(s, t)$	force vector in continuous domain
$\{F(t)\}$	force vector in discrete domain
$\{F_0\}$	initial force vector
G	shear modulus
h	depth of the beam
KE	kinetic energy
$[K]$	stiffness matrix
$L[\ ]$	differential operator for stiffness
m	mass per unit length
M_y	internal moment about y- axis
$M[\ ]$	differential operator for mass
$[M]$	mass matrix
n	number of grids
N	internal normal force, number of element or number of time interval
$\{q_0\}$	initial displacement vector
$\{q_1\}$	displacement vector at time t_1
$\{q_{j+1}\}$	displacement vector at time t_{j+1}
$\{q(t)\}$	displacement vector
R_0	radius parameter of the catenary curve
s	circumferential coordinate

s_L	length of the beam
SE	strain energy
t	time
T	internal axial force
T_f	final time
$u(s, t)$	radial displacement
$w(s, t)$	tangential displacement
W_{nc}	work of the non-conservative forces
(x_r, z_r)	the tip co-ordinates of the curved beam
α, α_r	slope of the curve at any point and point r
α, β	Rayleigh damping coefficients
δ	variation operator or dirac delta function
Δt	time interval
ε	tangential strain due to tension
ρ	density of material of beam
κ_0'	initial curvature
κ_1'	curvature after displacement occurs
$\rho_0(z), \rho_0(\alpha), \rho_0(s)$	variable radius of curvature
ω	natural frequency
(`)	derivative with respect to “s”
(.)	derivative with respect to “t”

CHAPTER 1

GENERAL INTRODUCTION

Curved beams can be seen a lot of applications such as stiffeners in airplane/ship/roof structures. They can be in the shape of a space curve or a plane curve, and also have variable curvature and cross-section. Their geometrical properties are basically related with the functional and esthetical requirements.

Curved beams have two types of motions for in-plane vibrations: (1) bending, (2) extensional or axial. Bending and axial motions are coupled. In order to uncouple the equations for in plane vibration, inextensionality condition can be used. This condition necessitates zero axial strain in neutral axis.

There are many studies for vibrations of the curved beams, but only a few studies for curved beams with variable curvature. The selected studies are introduced in the order of publication time as follows:

Den Hartog (1928) derived formulae for the first and second natural frequencies of a part of a circular ring, hinged or clamped at its ends. He shown that the type of vibration, in which extension of the fibers occurs, under certain conditions may have a lower natural frequency than the non-extensional type of vibration.

Volterra and Morell (1960) extended the study of Den Hartog (1928). They analyzed the free vibration of arches with various geometries such as circle, cycloid, catenary, and parabola by using the Rayleigh-Ritz method.

Romanelli and Laura (1972) calculated the lowest natural frequencies of elastic hinged arcs by using Rayleigh's principle. Since they derived the energy equation for non-circular arcs, they also criticized the bending moment equation given by Volterra and Morell (1960).

Wang (1972) used the Rayleigh-Ritz method to find the lowest natural frequency of clamped parabolic arcs to see the effect of the variation of depth and width on natural frequencies.

Wang and Moore (1973) analyzed the lowest natural extensional frequency of symmetrical elliptic arcs with clamped-clamped ends by using the Rayleigh-Ritz method.

Takahashi et al (1977) researched the in-plane vibrations of curved beam of which the center line of an ellipse or of a sinus curve. They used two methods to solve the problem: in first one, curvature function is expressed in terms of arch length, in second one, arch length function is expressed in terms of curvature.

Sakiyama (1985) presented an approximate method to analyze the free vibration of any type of arches. The solutions of differential equations were obtained in discrete form, by translating the differential equations into integral equations and applying numerical integrations.

Lee and Wilson (1989) derived the equations for in-plane vibrations of variable curvature arches in parabolic, sinusoidal and elliptic geometries. They solved the equations numerically for frequencies and mode shapes. They also validated the lowest four predicted frequencies and mode shapes for parabolic arches experimentally.

Gutierrez et al. (1989) calculated only the lowest natural frequencies in flexure and extension for non-circular arches with variable cross-section by using polynomial approximations and the Ritz method.

Taking into account the shear deformation and rotary inertia, Yıldırım (1997) computed the in-plane and out-of-plane free vibration frequencies of Archimedes-type spirals shown in Figure 1.1 by using the transfer matrix method. To compute the overall dynamic transfer matrix, she used the complementary functions method and concluded that the solution method can be applied to any planar bar.

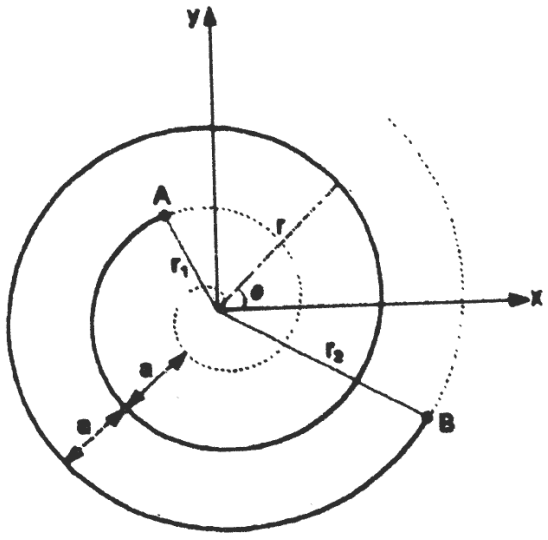

Figure 1.1. Archimedes-type spiral spring
(Source: Yıldırım 1997)

Huang et al (1998a) developed an exact solution for in plane vibration of arches with variable curvature as well as cross section by using Frobenius method combined with dynamic stiffness method. Shear deformation and rotary inertia effects are considered. They provided some non-dimensional frequencies of parabolic arches in tables and graphic charts based on the rise to span length, slenderness ratio, and variation of cross section.

Oh et al. (1999) derived the differential equations for free in-plane vibrations of non-circular arches of which one illustrated in Figure 1.2, including the rotatory inertia, shear deformation and axial deformation effects. Figure 1.2 also shows a small element of the arch defines the positive directions for its loads: the axial forces N, the shear forces Q, the bending moments M, the radial inertia force P_r, the tangential inertia force P_t and rotary inertia couple T. In order to obtain frequencies and mode shapes, they solved the differential equations numerically. The lowest four natural frequencies are calculated for the parabolic, elliptic and sinusoidal geometries with hinged-hinged, hinged-clamped, and clamped-clamped end conditions. A wide range of arch rise to span length ratios, slenderness ratios, and two different values of shear parameter are also considered. Their numerical results are in good agreement with results determined by means of finite element method.

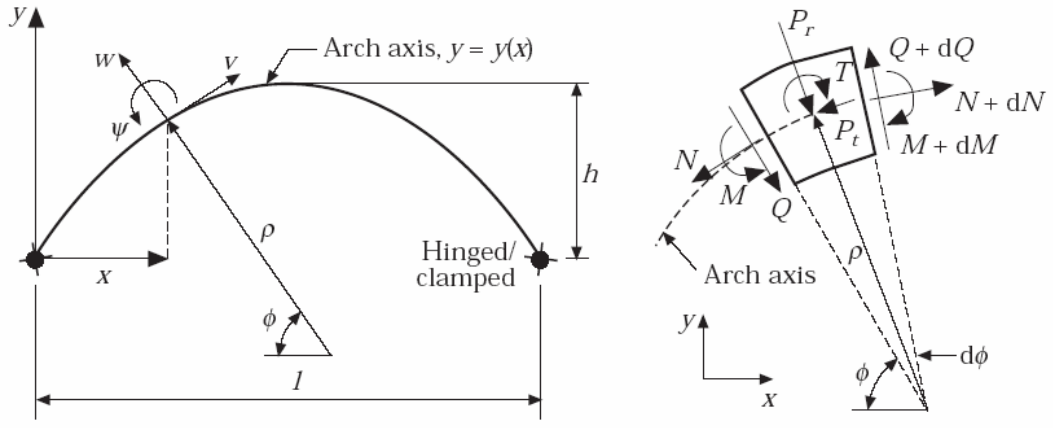

Figure 1.2. Arch geometry and loads on an arch element
(Source: Oh *et al*. 1999)

Oh et al. (2000) presented additionally experimental results for the free vibration frequencies and mode shapes of three quadratic parabolic arches. They concluded that

experimental measurements of frequencies and their corresponding mode shapes are close agreement with the predicted frequencies and their corresponding mode shapes.

There are a few studies for transient responses of curved beams with variable curvature under different type of loadings. Therefore, the reachable ones related with the transient responses of curved beams are mentioned below:

The oldest reachable literature on curved beam under impact load is a Master of Science study in Civil Engineering Department of the Georgia Institute of Technology in 1954. This study was completed by Arthur Remington White with thesis advisor Professor H.C. Saxe. The purpose of this investigation was two-fold; first to begin a study of the behavior of curved beams under dynamic loading, with special reference to arches in civil engineering use. The secondary purpose is to begin the study of structural dynamics in the Civil Engineering Department of the Georgia Institute of Technology by establishing experimental techniques. Four factors were analyzed:

(1) The maximum stress during impact,

(2) The length of time the striking mass is in contact the model,

(3) The natural frequencies of the bar,

(4) The modes of full vibration of the bar.

The study leads to the follow conclusions:

(l) Conventional theory gives good results for the maximum stress during impact,

(2) The time of contact may be predicted with good accuracy by common methods,

(3) The approximate theory of free vibrations of curved bars gives an accurate analysis for bars of small central angles.

Sheinman (1979) published a paper on a generalization of the dynamic solution for an arbitrary plane curved beam with viscous damping, under arbitrary load. The equation of motion, based on the linear theory, admits proportionality of the damping to the mass and stiffness matrices (Raleigh damping). The numerical solution is obtained by direct time-integration, using backward differences (Houbolt's method). A general computer program (CURBEAM) was written for this purpose and a numerical example is presented.

Yu et al. (1985) published another paper on a quadrantal circular curved cantilever beam struck in its plane at its tip by a rigid mass moving radially at an initial speed VO, as shown in Figure 1.1. If the impact duration is very short and the rigid mass adheres to the beam after impact, the load pulse may be idealized as impulsive, i.e. of 8-function pulse shape. Treating the mass as a particle, the problem then to be analyzed is that of a curved-beam-lumped-mass system with a specified initial velocity at the mass towards the centre

of the quadrant. An 'exact' rigid-plastic solution will be constructed first. This will then be compared with a simpler complete solution, with a mode approximation solution, and with an elastic-plastic numerical solution by using the finite element code ABAQUS. Bounds on displacement and response time according to rigid-plastic theory are also computed and presented.

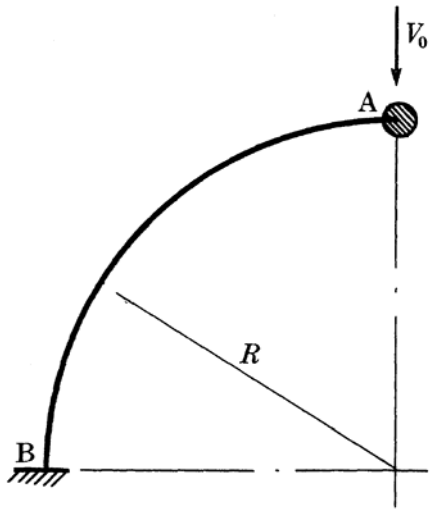

Figure 1.3. A quadrantal circular beam subjected to radial impact in its own plane at its tip by a rigid mass.(Source: Yu et al. 1985)

Huang and Tseng (1996) analytically analyzed in plane transient response of a circular arch subjected to a point loading and support motions load by Laplace transform.

Huang et al (1998b) proposed a procedure combining the dynamic stiffness method with the Laplace transform to obtain accurate transient responses of an arc with variable curvature. They also considered the effects of shear deformation, rotary inertia, and damping in the proposed procedure. A parabolic and a semi elliptic arch subjected to either point loading or base excitation are presented as examples.

Marur and Kant (2011) proposed a higher order refined model with isoparametric elements to study the transient dynamic response of laminated arches/curved beams. They solved the equation of motion by Newmark integration scheme and validated the higher order formulation with available results and subsequently applied to arches with various curvatures, aspect ratios, boundary conditions, loadings and lamination schemes.

Bhatti and Kishi (2011) simulated impact-response analysis RC arch-type beams without stirrups by conducting falling weight impact loading tests of small-scale arch-shape RC beams shown in Figure 1.4. Since the preparing of specimens and fitting of experimental setup are difficult, they performed numerical simulation methods by using

computers in addition to the experiments of which set up shown in Figure 1.5. They obtained the impact force time history, maximum displacement at the loading point and crack patterns caused in the side-surface of the arch beams.

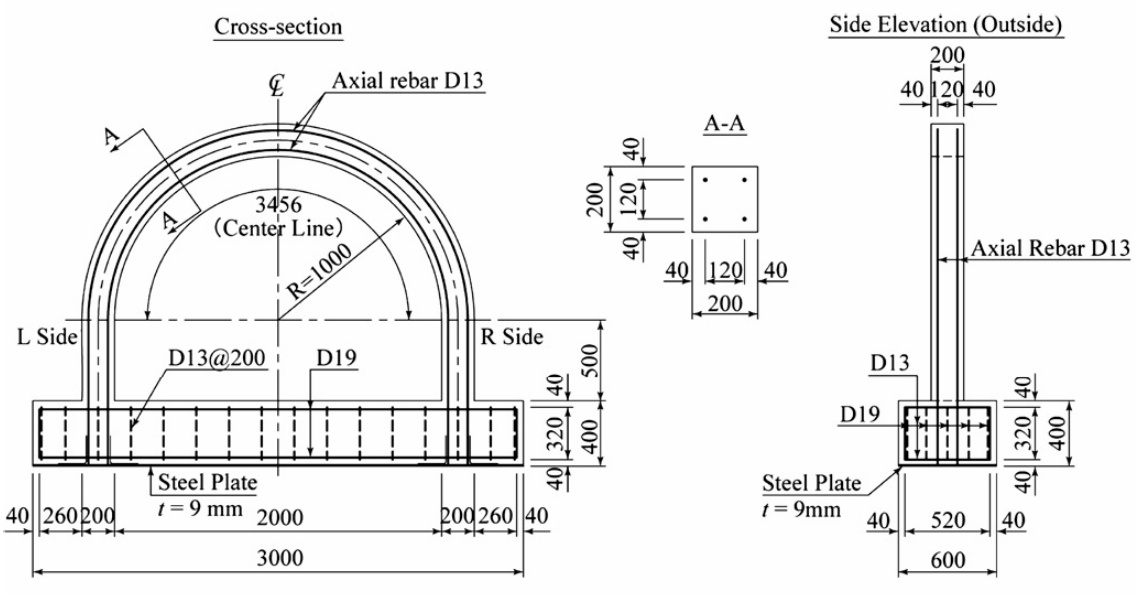

Figure 1.4. Dimensions of the RC arch beam model
(Source: Bhatti and Kishi 2011)

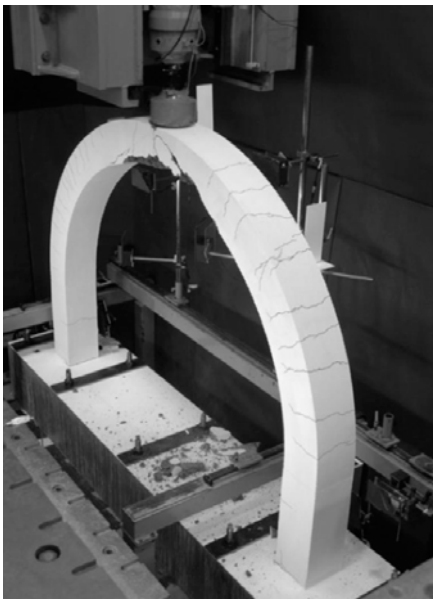

Figure 1.5. Pictorial view of the experimental setup
(Source: Bhatti and Kishi 2011)

Recently, Nikkhoo and Kananipour (2014) proposed a dynamic numerical solution for deflections of semicircular curved beams acted upon by moving loads. They used the

Euler–Bernoulli beam theory considering polar system, in order to extract the characteristic equations of an arch under an in-plane constant moving load, then solved it by using differential quadrature method. The obtained results are radial and tangential displacements, as well as bending moments. Confirmation of this approach, some comparisons have been made between the results obtained by selected methods such as differential quadrature method, Galerkin method, and finite element method. The results show differential quadrature method is efficient.

In this study, time response of a planar curved beam in the shape of catenary under in-plane impact load is analyzed by Finite Difference and Finite Element Methods. The main mathematical problems are to find the eigenvalues and to obtain the time response. A computer program is developed in Mathematica for the solution with Finite Difference Method. On the other hand, a computer code is written for the geometric and finite element models of curved beam with variable curvature in ANSYS by using APDL (ANSYS Parametric Design Language). Solutions of the two methods are compared in each other and then good agreement is observed. The effects of impuls and damping properties on the time response are investigated.

CHAPTER 2

THEORETICAL VIBRATION ANALYSIS

2.1. Introduction

A planar curved beam with variable radius of curvature shown in Figure 2.1 is considered. A catenary form is selected for the curved beam axis. Formulations about catenary form are presented in the next section. Since the Hamilton principle is very powerful method for the derivation of equation of motion in continuous system, equation of motion and related boundary conditions for in-plane vibrations of curved beam with variable curvature are obtained by the Hamilton principle in the following section. Since the problem presented in abstract is based on *differential eigenvalue problem* with variable coefficients and the *initial value problem associated with particular solution*, the solution of the problem has two main steps. Due to the variable coefficients in the equation of motion, numerical solution is required. Therefore, discretization of continuous systems can be accomplished by two methods to validate the results: Finite Difference and Finite Element. Transient analysis by Finite Difference Method is based on direct integration methods (Cook 1989). On the other hand, transient analysis with Finite Element Method provided by ANSYS is presented for three methods: full, reduced and mode superposition. Three sample input listings for the methods given above are shown.

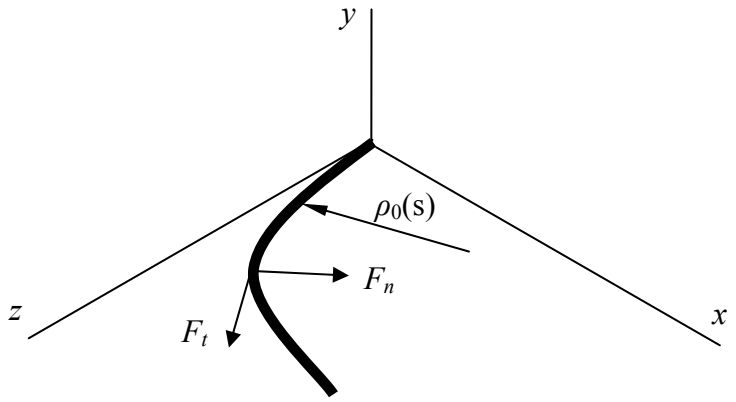

Figure 2.1. A planar curved beam with variable radius of curvature under impact loads.

2.2. Geometry of Curved Beam

The catenary curve and its parameters are shown in Figure 2.2. The necessary equations are given by Yardimoglu (2010) as follows:

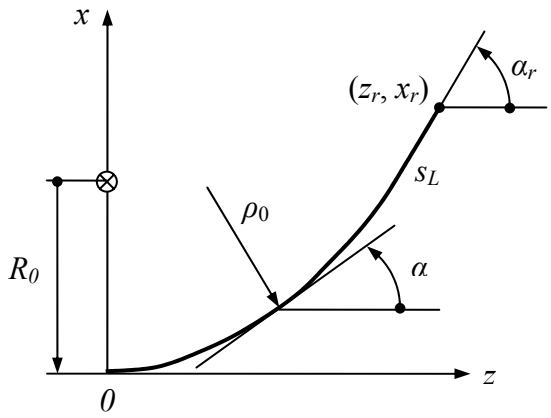

Figure 2.2. Parameters of catenary beam
(Source: Yardimoglu 2010)

The catenary curve is expressed in *x*-*z* plane in terms of *x* and *z* as follows:

$$x(z) = R_0[\cosh(z / R_0) - 1] \tag{2.1}$$

The slope α at abscissa *z* is obtained by differentiation of Equation 2.1 with respect to *z*:

$$\tan\alpha = dx(z) / dz = \sinh(z / R_0) \tag{2.2}$$

The tip co-ordinates (z_r, x_r) of the curved beam is obtained by using the tip slope α_r as

$$z_r = R_0 \, arc\sinh(\tan\alpha_r) \tag{2.3}$$

$$x_r = R_0 \, (1/\cos\alpha_r - 1) \tag{2.4}$$

Since the arc length *s* from origin 0 to any point (z, x) on the curve is

$$s(z) = \int_0^s \sqrt{(1 + (dx(z)/dz)^2}\, dz = R_0 \tan\alpha \tag{2.5}$$

Equation 2.5 gives a relationship between s and α. Moreover, radius of curvature at abscissa z is found by using the well-known radius of curvature eqaution as follows:

$$\rho_0(z) = \frac{\left[1 + (dx(z)/dz)^2\right]^{3/2}}{d^2x(z)/dz^2} = R_0 \cosh^2(z/R_0) \tag{2.6}$$

Eliminating the variable z in Equation 2.6 by using Equation 2.2, radius of curvature can be written in terms of α as follows:

$$\rho_0(\alpha) = R_0 / \cos^2\alpha \tag{2.7}$$

Now, cos α can be expressed in terms of s by using Equation 2.5 as

$$\cos\alpha = R_0 / \sqrt{R_0^2 + s^2} \tag{2.8}$$

Therefore, radius of curvature can also be written in terms of s as follows:

$$\rho_0(s) = R_0 + s^2 / R_0 \tag{2.9}$$

2.3. Derivation of the Equation of Motion

The present curved beam is shown in Figure 2.3.

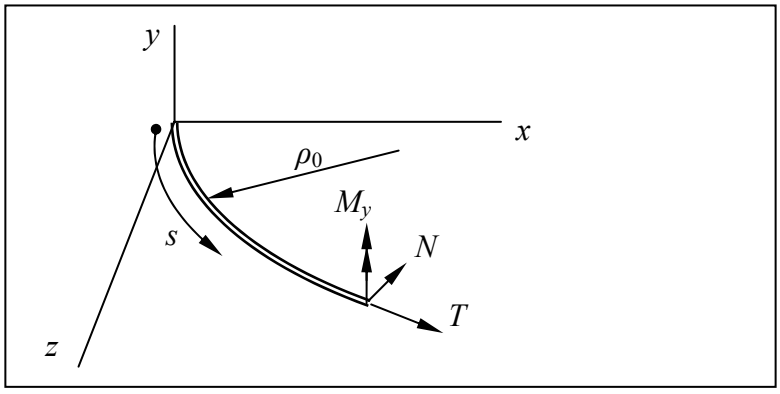

Figure 2.3. A curved beam with internal forces and moments

It can be seen from Figure 2.3 that N, T and M_y are internal normal and shear forces and bending moment, respectively. Displacements of any point on curved beam in x and z directions are denoted by u and w, as usual. Dynamic curvature κ_1' in x-z plane is given by Love (1944) as

$$\kappa_1' = \kappa_0' + \frac{d}{ds}\left(\frac{du}{ds} + \kappa_0' w\right) \tag{2.10}$$

where κ_0' is initial curvature or static curvature. Axial force T is given as (Love 1944)

$$T = E A \varepsilon \tag{2.11}$$

where ε is tangential strain due to tension and expressed as

$$\varepsilon = \frac{dw}{ds} - \kappa_0' u \tag{2.12}$$

Bending moment M_y is written as follows

$$M_y = B(\kappa_1' - \kappa_0') \tag{2.13}$$

where B is bending rigidity of curved beam material, generally expressed as EI.

The Hamilton principle is expressed as follows (Meirovitch 2001):

$$\delta \int_{t_1}^{t_2} (KE - SE + W_{nc})\, dt = 0 \tag{2.14}$$

where KE, SE and W_{nc} are the kinetic, strain energies and the work of the non-conservative forces, respectively. For the present problem, they are given as follows;

$$KE = \frac{1}{2}\int_0^{S_L} (m\dot{u}^2 + m\dot{w}^2)\, ds \tag{2.15}$$

where $m = \rho A$ is mass per unit length, in which A is area of the cross-section.

$$SE = \frac{1}{2}\int_0^{S_L} M_y\,(\kappa_1' - \kappa_0')\,ds \tag{2.16}$$

By using Equation 2.13 along with Equation 2.10 in Equation 2.16, the following strain energy expression is obtained:

$$SE = \frac{1}{2}\int_0^{S_L} (B[\frac{d^2u}{ds^2} + \frac{d}{ds}(\kappa_0' w)]^2\,ds \tag{2.17}$$

$$W_{nc} = \frac{1}{2}\int_0^{S_L} (F_n\,\delta(s - s_L/2)\,u + F_t\delta(s - s_L/2)w)\,ds \tag{2.18}$$

where F_n and F_t are external forces acting in normal and tangential directions, respectively, as shown in Figure 2.1. $\delta(s\text{-}s_L/2)$ is a spatial Dirac delta function applied at s=$s_L/2$ and defined as (Meirovitch 2001)

$$\delta(s - s_L/2) = 0 \qquad , \qquad s \neq s_L/2 \tag{2.19}$$

and

$$\int_0^{S_L} \delta(s - s_L/2)\,ds = 1 \tag{2.20}$$

If central line of curved beam is assumed as unextended, the inextensionality condition is obtained from Equation 2.12 as

$$\frac{dw}{ds} = u\kappa_0' \tag{2.21}$$

By substituting Equations 2.15, 2.17 and 2.18 along with Equation (2.21) in Equation 2.14, governing differential equations and the boundary conditions for the present problem are obtained as follows:

$$
\begin{aligned}
&f_6(s)\frac{\partial^6 w}{\partial s^6}+f_5(s)\frac{\partial^5 w}{\partial s^5}+f_4(s)\frac{\partial^4 w}{\partial s^4}+\\
&f_3(s)\frac{\partial^3 w}{\partial s^3}+f_2(s)\frac{\partial^2 w}{\partial s^2}+f_1(s)\frac{\partial w}{\partial s}+\\
&f_0(s)-\rho A\frac{\partial^2 w}{\partial t^2}-\frac{2\rho A}{\kappa_0'(s)^3}\frac{\partial \kappa_0'}{\partial s}\frac{\partial^3 w}{\partial s\partial t^2}+\\
&\frac{\rho A}{\kappa_0'(s)^2}\frac{\partial^4 w}{\partial s^2\partial t^2}=F_t-\frac{\partial(F_n/\kappa_0(s))}{\partial s}
\end{aligned}
\tag{2.22}
$$

where

$$
f_0(s)=B\kappa_0'(s)\frac{\partial^2\kappa_0'}{\partial s^2}-\frac{B}{\kappa_0'(s)^2}\frac{\partial\kappa_0'}{\partial s}\frac{\partial^3\kappa_0'}{\partial s^3}+\frac{B}{\kappa_0'(s)}\frac{\partial^4\kappa_0'}{\partial s^4} \tag{2.23.a}
$$

$$
\begin{aligned}
f_1(s)=&2B\kappa_0'(s)\frac{\partial\kappa_0'}{\partial s}-\frac{6B}{\kappa_0'(s)^3}\frac{\partial\kappa_0'^3}{\partial s}\\
&-\frac{144B}{\kappa_0'(s)^7}\frac{\partial\kappa_0'^5}{\partial s}+\frac{3B}{\kappa_0'(s)^2}\frac{\partial\kappa_0'}{\partial s}\frac{\partial^2\kappa_0'}{\partial s^2}\\
&+\frac{276B}{\kappa_0'(s)^6}\frac{\partial\kappa_0'^3}{\partial s}\frac{\partial^2\kappa_0'}{\partial s^2}-\frac{96B}{\kappa_0'(s)^5}\frac{\partial\kappa_0'}{\partial s}\frac{\partial^2\kappa_0'^2}{\partial s^2}\\
&+\frac{3B}{\kappa_0'(s)}\frac{\partial^3\kappa_0'}{\partial s^3}-\frac{68B}{\kappa_0'(s)^5}\frac{\partial\kappa_0'^2}{\partial s}\frac{\partial^3\kappa_0'}{\partial s^3}\\
&+\frac{20B}{\kappa_0'(s)^4}\frac{\partial^2\kappa_0'}{\partial s^2}\frac{\partial^3\kappa_0'}{\partial s^3}+\frac{11B}{\kappa_0'(s)^4}\frac{\partial\kappa_0'}{\partial s}\frac{\partial^4\kappa_0'}{\partial s^4}\\
&-\frac{B}{\kappa_0'(s)^3}\frac{\partial^5\kappa_0'}{\partial s^5}
\end{aligned}
\tag{2.23.b}
$$

$$
\begin{aligned}
f_2(s)=&B\kappa_0'(s)^2+\frac{3B}{\kappa_0'(s)^2}\frac{\partial\kappa_0'^2}{\partial s}+\frac{144B}{\kappa_0'(s)^6}\frac{\partial\kappa_0'^4}{\partial s}\\
&+\frac{3B}{\kappa_0'(s)}\frac{\partial^2\kappa_0'}{\partial s^2}-\frac{204B}{\kappa_0'(s)^5}\frac{\partial\kappa_0'^2}{\partial s}\frac{\partial^2\kappa_0'}{\partial s^2}\\
&+\frac{30B}{\kappa_0'(s)^4}\frac{\partial^2\kappa_0'^2}{\partial s^2}+\frac{44B}{\kappa_0'(s)^4}\frac{\partial\kappa_0'}{\partial s}\frac{\partial^3\kappa_0'}{\partial s^3}\\
&-\frac{5B}{\kappa_0'(s)^3}\frac{\partial^4\kappa_0'}{\partial s^4}
\end{aligned}
\tag{2.23.c}
$$

$$f_3(s) = -\frac{72B}{\kappa_0'(s)^5}\frac{\partial \kappa_0'^3}{\partial s} + \frac{66B}{\kappa_0'(s)^4}\frac{\partial \kappa_0'}{\partial s}\frac{\partial^2 \kappa_0'}{\partial s^2} - \frac{10B}{\kappa_0'(s)^3}\frac{\partial^3 \kappa_0'}{\partial s^3} \tag{2.23.d}$$

$$f_4(s) = 2B + \frac{24B}{\kappa_0'(s)^4}\frac{\partial \kappa_0'^2}{\partial s} - \frac{10B}{\kappa_0'(s)^3}\frac{\partial^2 \kappa_0'}{\partial s^2} \tag{2.23.e}$$

$$f_5(s) = -\frac{6B}{\kappa_0'(s)^3}\frac{\partial \kappa_0'}{\partial s} \tag{2.23.f}$$

$$f_6(s) = \frac{B}{\kappa_0'(s)^2} \tag{2.23.g}$$

The boundary conditions are as follows:

a) Either bending moment is zero (pinned or free), or slope is zero (clamped).

b) Either shear force is zero (free), or displacement is zero (pinned or clamped).

c) Either bending moment is zero (pinned or free), or displacement is zero (pinned or clamped).

2.4. Discretization of Continuous Systems

2.4.1. Finite Difference Method for Transient Analysis

Transient analysis is also called time-history analysis. This analysis is interested in the dynamic response of a structure under the effect of dynamic loads. Dynamic response may be the time-dependent displacements, strains, stresses, and forces in a structure.

The partial differential equation for the forced vibration of a damped continuous system is given by Yardimoglu (2012) as follows,

$$M[\ddot{w}(s,t)] + C[\dot{w}(s,t)] + L[w(s,t)] = F(s,t) \tag{2.24}$$

where $M[\ ]$, $C[\ ]$, and $L[\ ]$ are linear differential operators having derivatives with respect to s and $F(s, t)$ is external loading.

In the FDM, the derivatives of dependent variables $w(s, t)$ in Equation 2.24 with respect to s are replaced by the finite difference approximations at mesh points shown in Figure 2.3. Therefore, the following matrix equation is obtained:

$$[M]\{\ddot{q}(t)\} + [C]\{\dot{q}(t)\} + [K]\{q(t)\} = \{F(t)\} \tag{2.25}$$

where $\{q(t)\}$ is the displacement vector obtained by discretizing $w(s, t)$ at the mesh points. Similarly, $\{F(t)\}$ is the force vector obtained by discretizing $F(s, t)$ at the mesh points. Moreover, $[K]$, $[M]$, and $[C]$ are stiffness, mass and damping matrices, respectively.

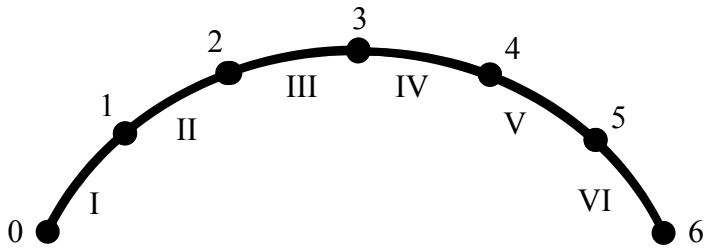

Figure 2.4. A curved domain divided into six sub domains.
(Source: Cangar 2013)

If the damping matrix $[C]$ is linear combination of stiffness matrix $[K]$ and mass matrix $[M]$, damping is called as Rayleigh damping and expressed as (Inman, 2001):

$$[C] = \alpha\ [M] + \beta [K] \tag{2.26}$$

where α and β are constant coefficients. It is also called proportional damping.

If the coefficients α and β are known, the following equation is used to determine the modal damping ratio ξ_i

$$\xi_i = 0.5(\alpha / \omega_i + \beta\omega_i) \qquad i = 1,2,.....n \tag{2.27}$$

where ω_i is the i-th natural frequency of the system. On the other hand, if the modal damping ratios ξ_m and ξ_n associated with two specific frequencies (modes) ω_m, ω_n are known, the coefficients α and β can be found by using Equation (2.26) as (Clough 2003)

$$\begin{bmatrix} \alpha \\ \beta \end{bmatrix} = 2\frac{\omega_m \omega_n}{\omega_n^2 - \omega_m^2} \begin{bmatrix} \omega_n & -\omega_m \\ -1/\omega_n & 1/\omega_m \end{bmatrix} \begin{bmatrix} \xi_m \\ \xi_n \end{bmatrix} \tag{2.28}$$

Where ω_m is the fundamental frequency. Since the variation of damping ratio with frequency rarely is available, it is assumed that $\xi_m = \xi_n = \xi$. Therefore,

$$\begin{bmatrix} \alpha \\ \beta \end{bmatrix} = \frac{2\xi}{\omega_m + \omega_n} \begin{bmatrix} \omega_m \omega_n \\ 1 \end{bmatrix} \tag{2.29}$$

Transient analysis can be performed by direct integration methods or step-by-step methods (Cook 1989). In this method, again finite difference approximation is used to replace the time derivatives appearing in Equation (2.25).

This method has the advantage that the frequencies and modes of free vibration of the undamped system do not have to be calculated prior to the response analysis. In order to evaluate the response at time T_f, the time interval (0, T_f) is divided into N equal time intervals $\Delta t = T_f / N$. The response is then calculated at the times Δt, $2\Delta t$, $3\Delta t$, . . . , T_f, by an approximate technique. The error in these approximations is of the order $(\Delta t)^2$. The procedure is outlined below (Petyt 2010):

First, solve the following equation

$$[M]\{\ddot{q}_0\} + [C]\{\dot{q}_0\} + [K]\{q_0\} = \{F_0\} \tag{2.30}$$

for the acceleration vector $\{\ddot{q}_0\}$. Second, calculate $\{q_1\}$ by using the next equation:

$$\{q_1\} = \{q_0\} + \Delta t\{\dot{q}_0\} + ((\Delta t)^2 / 2)\{\ddot{q}_0\} \tag{2.31}$$

Then, calculate the $\{q_{j+1}\}$ starting with j=1, from the following equation

$$\begin{aligned}&\left(1/(\Delta t)^2[M]+1/(2\Delta t)[C]\right)\{q_{j+1}\}\\&=\{F_j\}+\left(2/(\Delta t)^2[M]-[K]\right)\{q_j\}\\&\quad-\left(1/(\Delta t)^2[M]-1/(2\Delta t)[C]\right)\{q_{j-1}\}\end{aligned}\tag{2.32}$$

until desired time T_f. Selection of the value of Δt is critical for numerical stability and accuracy. For good accuracy, it is selected as twenty times of natural period (Petyt 2010).

2.4.2. Finite Element Method for Transient Analysis

By using the Finite Element Method (Petyt 2010), Equation 2.24 is reduced to multi-degree-of-freedom system. Therefore equation of motion of the system is given by

$$[M]\{\ddot{q}(t)\}+[C]\{\dot{q}(t)\}+[K]\{q(t)\}=\{F(t)\}\tag{2.33}$$

In order to perform the transient analysis in this thesis, the common commercial software ANSYS is used. The ANSYS program uses the Newmark time integration method or an improved method called HHT to solve these equations at discrete time points. Three methods are available to do a transient dynamic analysis: *full, mode superposition,* and *reduced* (ANSYS 2004). The methods are summarized below.

2.4.2.1. Full Solution Method

The full method uses the full system matrices to calculate the transient response. It allows all types of nonlinearities such as plasticity, large deflections, large strain, and so on. Time stepping procedure is used automatically to determine the time step size required for each time step. Nonzero initial conditions are input either directly or by performing a static analysis load step(s) prior to the start of the transient itself.

A sample input listing for a full transient analysis is shown below:

```
!  Build the Model
/PREP7                    ! Enter PREP7
---...                    ! Generate model
FINISH
```

```
!  Apply Loads and Obtain the Solution
/SOLU                       ! Enter SOLUTION
ANTYPE,TRANS                ! Transient analysis
TRNOPT,FULL                 ! Full method
D,...                       ! Constraints
F,...                       ! Loads
SF,...
ALPHAD,...                  ! Mass damping
BETAD,...                   ! Stiffness damping
KBC,...                     ! Ramped or stepped loads
TIME,...                    ! Time at end of load step
AUTOTS,ON                   ! Auto time stepping
DELTIM,...                  ! Time step size
OUTRES,...                  ! Results file data options
LSWRITE                     ! Write first load step
---...                     ! Loads, time, etc. for 2nd load step
---...                     !
LSWRITE                     ! Write 2nd load step
SAVE
LSSOLVE,1,2                 ! Initiate multiple load step solution
FINISH
```

2.4.2.2. Reduced Solution Method

The reduced solution method uses reduced structure matrices based on the sub-structuring technique solve the time-dependent equation of motion for linear structures. The solution method imposes the following additional assumptions and restrictions:

1. Constant [M] and [K] matrices. This implies no large deflections or change of stress stiffening, as well as no plasticity, creep, or swelling.
2. Constant time step size Δt.
3. No element load vectors. This implies no pressures or thermal strains. Only nodal forces applied directly at master DOF (Degrees Of Freedom) or acceleration effects acting on the reduced mass matrix are permitted.
4. Nonzero displacements may be applied only at master DOF.

This method usually runs faster than the full transient dynamic analysis. A sample input listing for a reduced transient analysis is shown below:

```
!  Build the Model
/PREP7                  ! Enter PREP7
---                     ! Generate model
FINISH

!  Apply Loads and Obtain the Solution
/SOLU
ANTYPE,TRANS            ! Transient dynamic analysis
TRNOPT,REDUC            ! Reduced transient analysis
DELTIM,...              ! Integration time step sizes
```

```
M,...                   ! Master DOF
D,...                   ! Constraints
OUTRES,...              ! Results-file data controls
F,...                   ! Force = 0 at Time = 0
SOLVE
TIME,...                ! Time at end of second load step
F,...                   ! Force at end of second load step
SOLVE

FINISH
```

2.4.2.3. Mode Superposition Solution Method

The mode superposition method uses the natural frequencies and mode shapes of a linear structure to predict the response to transient forcing functions. This solution method imposes the following additional assumptions and restrictions:

1. Constant [K] and [M] matrices. This implies no large deflections or change of stress stiffening, as well as no plasticity, creep, or swelling.
2. Constant time step size Δt.
3. There are no element damping matrices. However, various types of system damping are available.
4. Time varying imposed displacements are not allowed.

A sample input listing for this method is shown below:

```
!  Build the Model
/PREP7          ! Enter PREP7
---             ! Generate model
FINISH

!  Obtain the Modal Solution
/SOLU           ! Enter SOLUTION
ANTYPE,MODAL    ! Modal analysis
MODOPT,REDU     ! Reduced method
M,...           ! Master DOF
TOTAL,...
D,...           ! Constraints
SF,...          ! Element loads
ACEL,...
SAVE
SOLVE
FINISH

!  Obtain the Mode Superposition Transient Solution
/SOLU           ! Reenter SOLUTION
ANTYPE,TRANS    ! Transient analysis
TRNOPT,MSUP,... ! Mode superposition method
LVSCALE,...     ! Scale factor for element loads
```

```
F,...           ! Nodal Loads
MDAMP,...       ! Modal damping ratios
DELTIM,...      ! Integration time step sizes
LSWRITE         ! Write first LS which is solved statically at time=0
---             ! Loads, etc. for 2nd load step
TIME,...        ! Time at end of second load step
KBC,...         ! Ramped or stepped loads
OUTRES,...      ! Results-file data controls
LSWRITE         ! Write 2nd load step (first transient load step)
SAVE
LSSOLVE         ! Initiate multiple load step solution
FINISH
```

CHAPTER 3

NUMERICAL RESULTS AND DISCUSSION

3.1. Introduction

In this chapter, impulse response of a curved beam with variable curvature is studies by the following numerical methods: (a) FDM (Finite Difference Method), (b) FEM (Finite Element Method). Since there is no similar study in the available literature, the numerical results are compared with each other to check the present results.

A symbolic program is developed in Mathematica for the FDM. On the other hand, the geometry and finite element model of curved beam with variable curvature is generated in ANSYS by using APDL (ANSYS Parametric Design Language). BEAM3 which is 2-D Elastic Beam is selected to model the curved beam.

Three different fixed-fixed curved beams with R_o={80, 100, 120} mm, s_L=200 mm are considered as curve models. The geometrical models generated in ANSYS are shown in Figure 3.1.

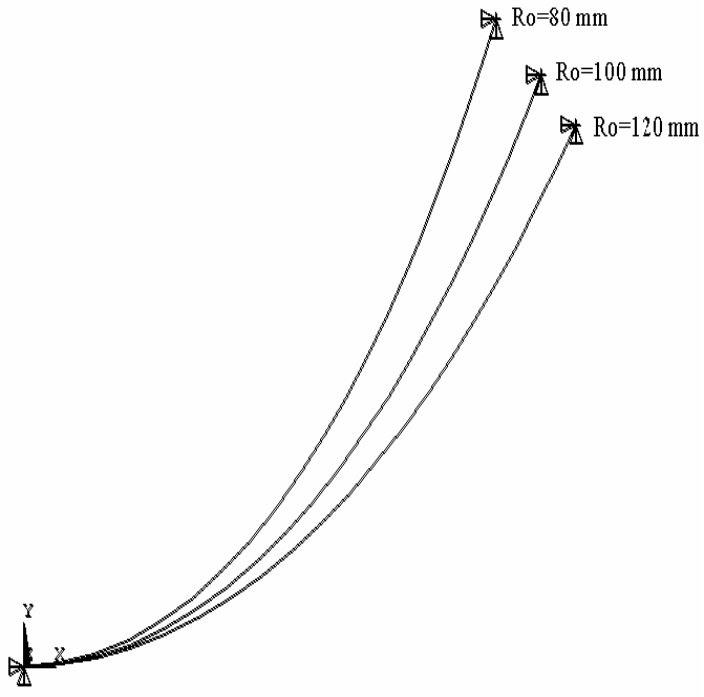

Figure 3.1. The three geometrical models of the curved beam

3.2. Convergence Studies for Natural Frequency

In order to decide the proper minimum number of grid point in FDM and number of element in FEM, the natural frequencies of a fixed-fixed curved beam with the parameters b=2 mm, h =8 mm, R_o=100 mm, s_L=200 mm are obtained for various discretizations. Material properties of curved beam are given in Table 3.1.

Table 3.1. Material properties in the models

E (MPa)	200000
ρ (ton/mm^3)	7.85 10^{-9}
G (MPa)	80000

The results are .given in Table 3.2 and Table 3.3 for FDM and FEM, respectively. From Table 3.2, the reasonable number of grid point n is selected as 100. Similarly, From Table 3.3, reasonable number of element N is selected as 20.

Table 3.2. Convergence of natural frequencies based on FDM

n	f_1 (Hz)
20	2085.08
40	2304.53
60	2383.4
80	2424.35
100	2449.48
120	2450.73

Table 3.3. Convergence of natural frequencies based on FEM

N	f_1 (Hz)
4	2504.3
6	2467.4
8	2457.3
10	2453.1
12	2450.9
14	2449.7
16	2448.9
18	2448.3
20	2447.9

Convergence of first natural frequency based on FDM is plotted in Figure 3.2. Also, convergence of first natural frequency based on FEM is plotted in Figure 3.2. It is seen from Figure 3.2 that the selected number of grid points and elements are reasonable.

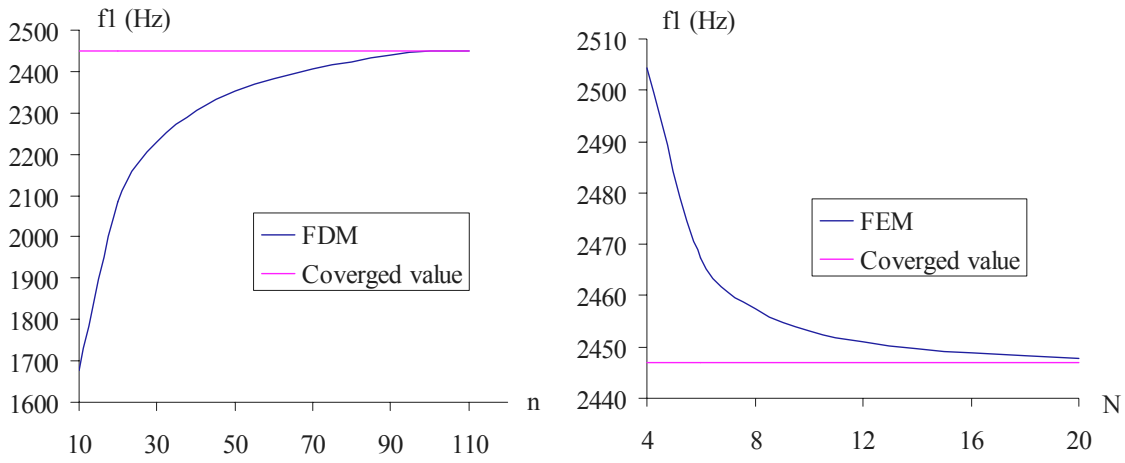

Figure 3.2. Convergence of first natural frequency by FDM and FEM

3.3. Natural Frequencies for Different Models

To see the effects of catenary curve parameter R_o and the height of the cross-section h of the curved beam on natural frequencies, various values for R_o and h are selected. The other parameters are b=2 mm, s_L=200 mm are taken. The results are given in Figures 3.2-3.5.

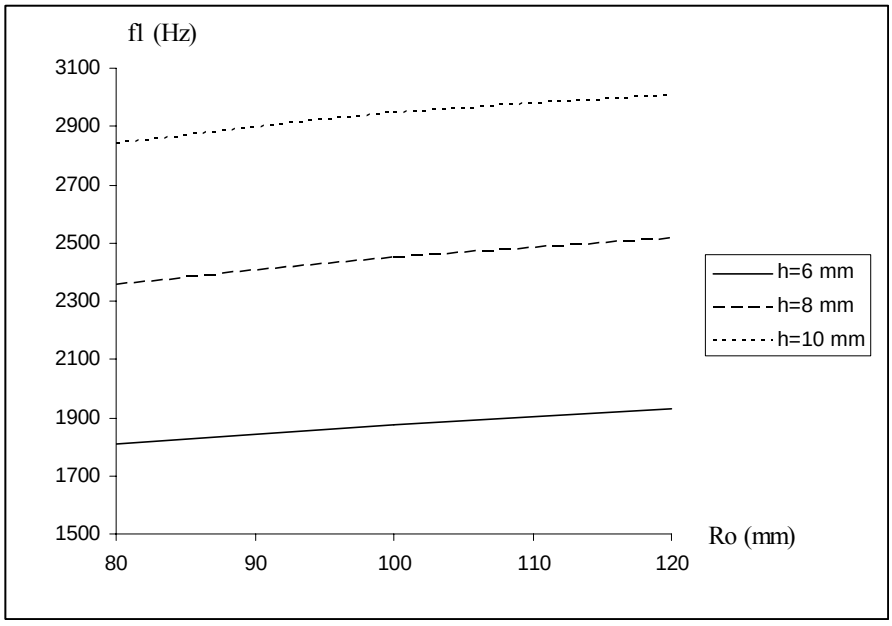

Figure 3.3. Effects of h and R_o on first natural frequencies

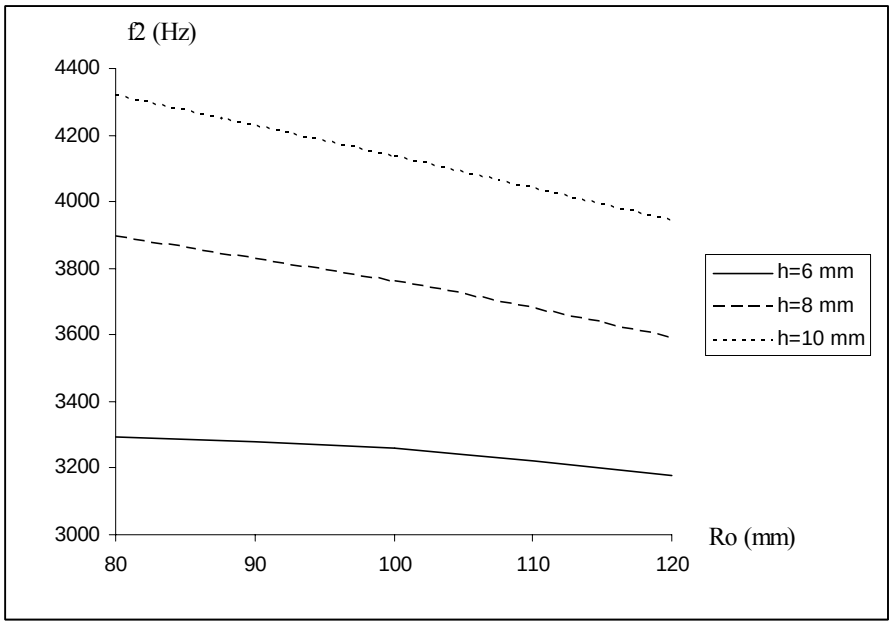

Figure 3.4. Effects of h and R_o on second natural frequencies

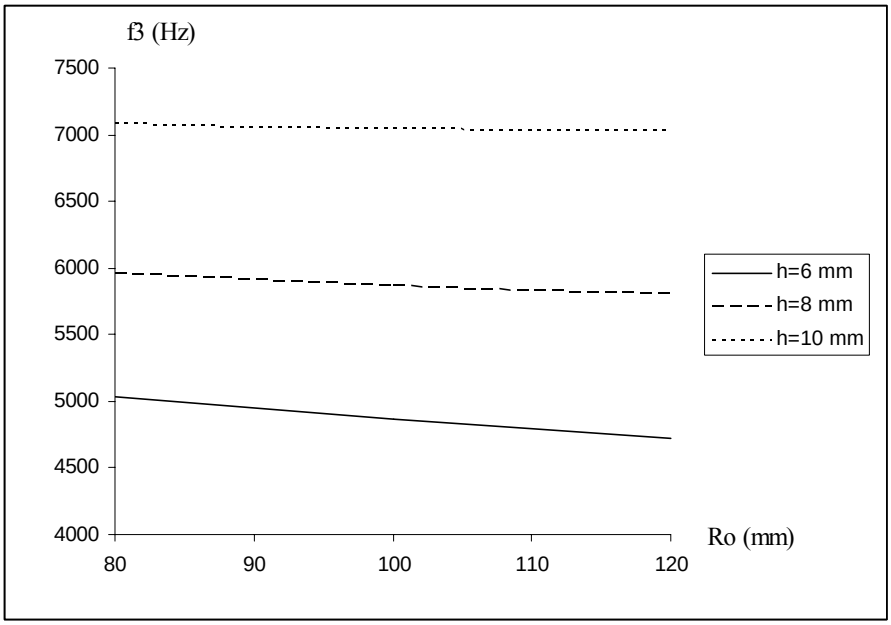

Figure 3.5. Effects of h and R_o on third natural frequencies

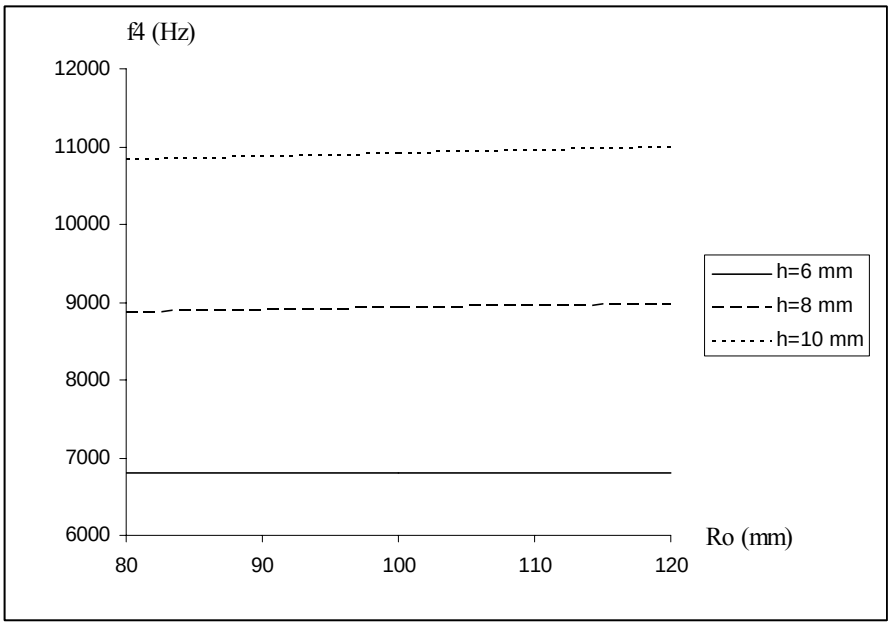

Figure 3.6. Effects of h and R_o on fourth natural frequencies

It can be seen from Figure 3.3 and 3.6 that when catenary parameter R_o increases for all depth of the beam h, first and fourth natural frequencies increase. Also, for a fixed value of R_o, when depth of the beam h increases, first and fourth natural frequencies increase. On the other hand, it can be seen from Figure 3.4 and 3.5 that the tendency of second and third natural frequencies reverse to the case in first and fourth natural frequencies when R_o increases.

3.4. Proportional Damping Parameters

Assuming the all the modal damping ratios are equal to each others, the coefficients α and β are calculated from Equation (2.29) for the damping ratio. Three different damping ratios $\{ \xi_a, \xi_b, \xi_c \}$ are considered. First, the coefficients $\alpha_a = \beta_a = 0$ are taken for $\xi_a=0$. Second, the coefficients $\alpha_b=932$ and $\beta_b=2.56\ 10^{-6}$ are found for $\xi_b=0.05$. Third, the coefficients $\alpha_c=1863.5$ and $\beta_c=5.13\ 10^{-6}$ are found for $\xi_c=0.1$.

3.5. Comparison Studies for Impact Response

Unit impact load at mid-point of the curved beam is applied at duration 2 ms. Time response of the curved beam of which parameters given in Section 3.2 with $\xi_b=0.05$ are given by FDM and FEM are given separately in Figure 3.7 and Figure 3.8, respectively.

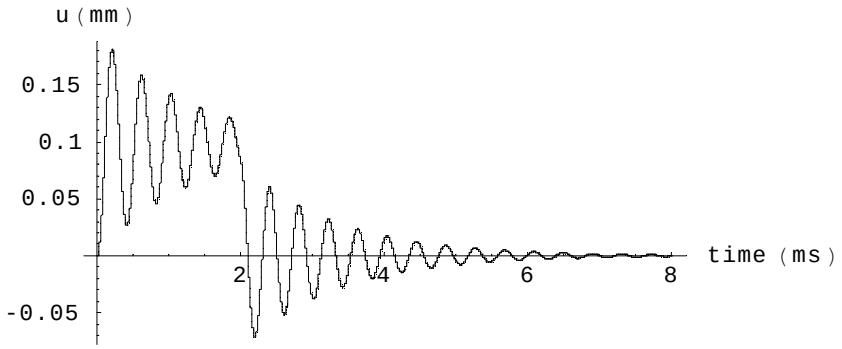

Figure 3.7. Time response for $\xi_b=0.05$ by FDM

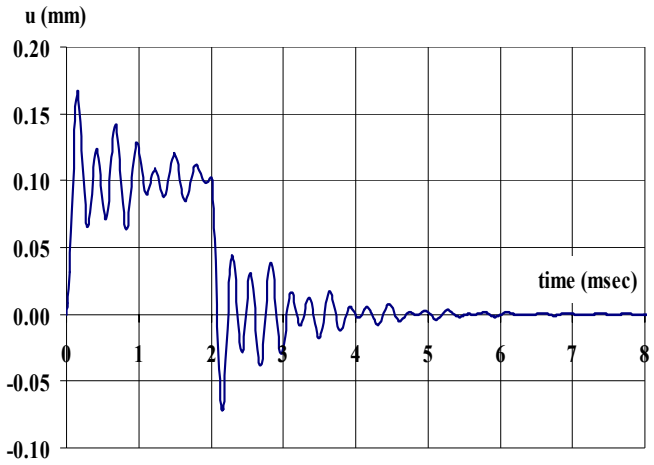

Figure 3.8. Time response for $\xi_b=0.05$ by FEM

In can be seen from Figure 3.7 and Figure 3.8 that in general both of them are in good agreement except FEM model damping tendency is not smooth as in FDM.

3.6. Impact Responses for Different Models

Up to this section, the necessary background for the displacement analysis of non-circular planar curved beams under in-plane impulsive load is obtained by:

- carrying out convergence studies for natural frequencies,
- finding the natural frequencies for different models based on the parameters set R_0={ 80, 100, 120} mm, h={ 6, 8, 10} mm.
- calculating the proportional damping parameters for selected three damping ratios ξ={ 0, 0.05, 0.1 }
- comparing the impact response plot obtained by FDM with the impact response plot obtained by FEM for ξ_b=0.05.

Therefore, in this section, impact responses for different models are presented considering model parameters based on the sets R_0={100, 120} mm, h={8, 10} mm, and ξ={0.05, 0.1}. For the sake of simplicity, the model numbers are given in Table 3.4.

Table 3.4. Parametric details of the models

Models number	s_L (mm)	b (mm)	h (mm)	R_o (mm)	ξ (-)
Model 1	200	2	8	100	0.05
Model 2	200	2	8	100	0.1
Model 3	200	2	8	120	0.05
Model 4	200	2	8	120	0.1
Model 5	200	2	10	100	0.05
Model 6	200	2	10	100	0.1
Model 7	200	2	10	120	0.05
Model 8	200	2	10	120	0.1

Time responses of Model 1 to Model 8 found by FDM are given in Figure 3.9 to Figure 3.16.

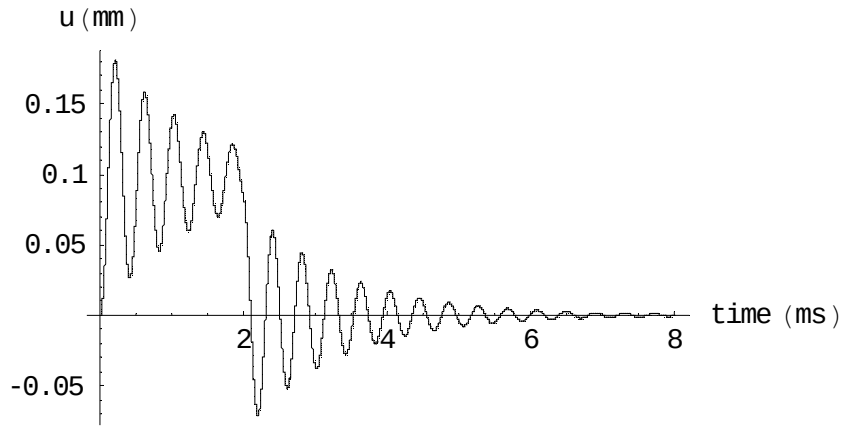

Figure 3.9. Time response for Model 1: h=8 mm, R_o=100 mm, ξ=0.05

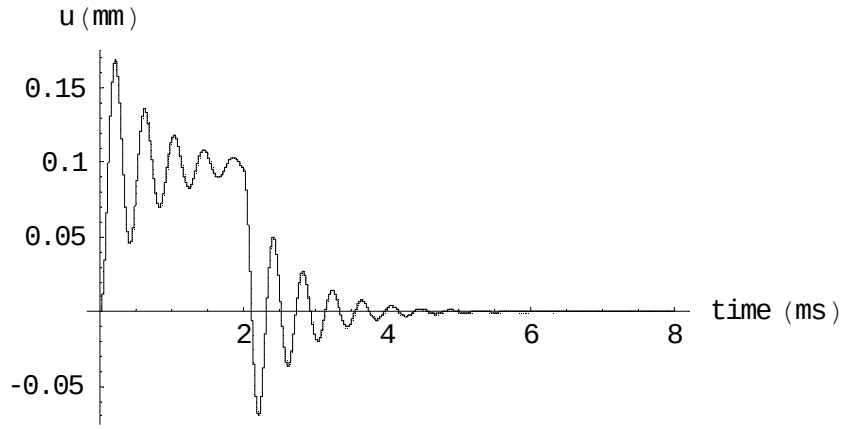

Figure 3.10. Time response for Model 2: h=8 mm, R_o=100 mm, ξ=0.1

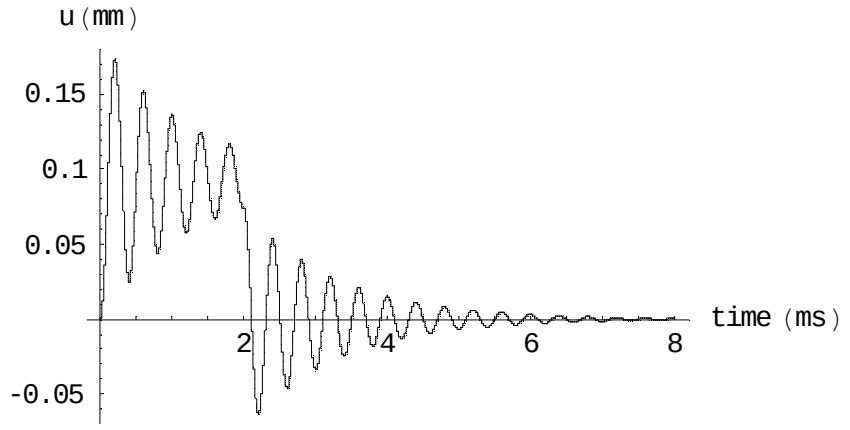

Figure 3.11. Time response for Model 3: h=8 mm, R_o=120 mm, ξ=0.05

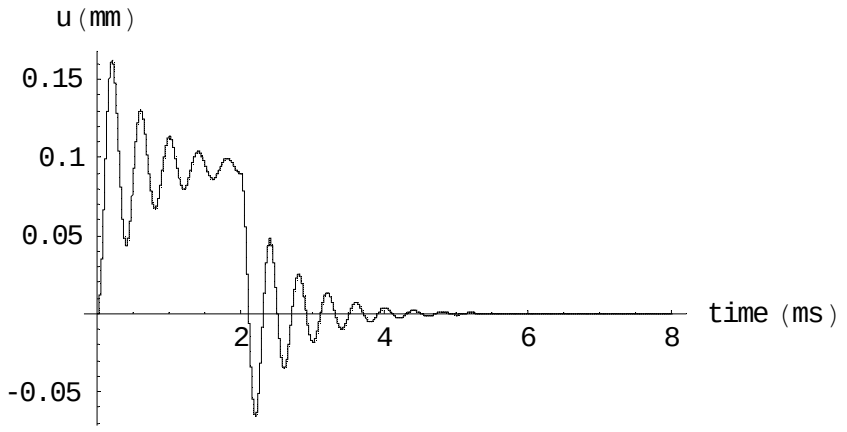

Figure 3.12. Time response for Model 4: h=8 mm, R_o=120 mm, ξ=0.1

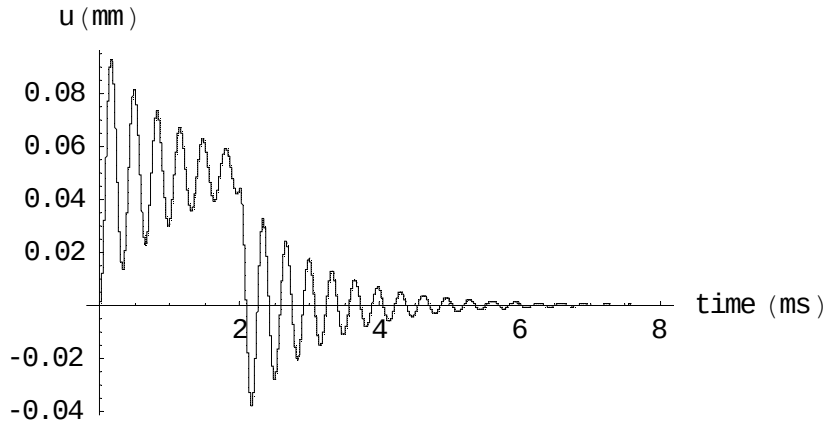

Figure 3.13. Time response for Model 5: h=10 mm, R_o=100 mm, ξ=0.05

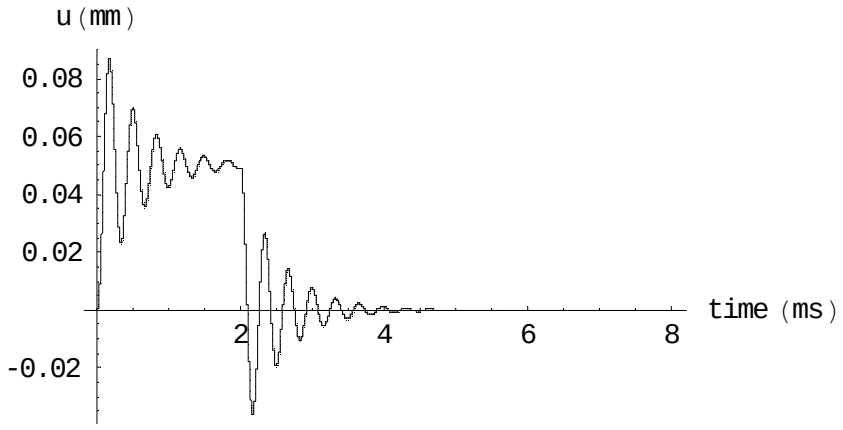

Figure 3.14. Time response for Model 6: h=10 mm, R_o=100 mm, ξ=0.1

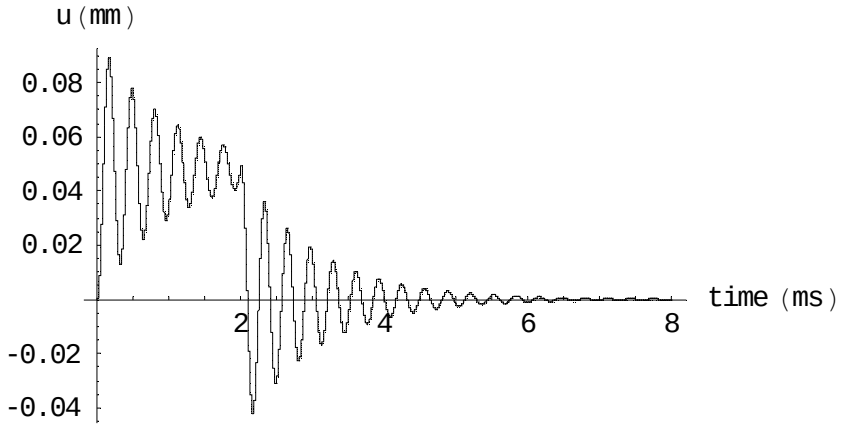

Figure 3.15. Time response for Model 7: h=10mm, R_o=120 mm, ξ=0.05

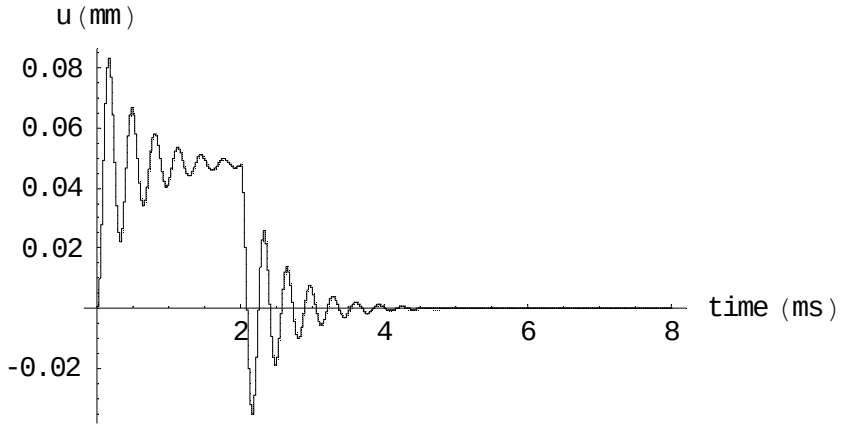

Figure 3.16. Time response for Model 8: h=10 mm, R_o=120 mm, ξ=0.1

The time response plots presented in the Figure 3.9 to Figure 3.16 are compared in each others, then the increasing and decreasing effects are given in tabular form in Tables 3.5 to 3.7.

Table 3.5. Comparisons of the model response in the form of $u(t) = U\sin(\omega t + \phi)$

Model	compared with Model	h	$u(t)$
1: h=8, R_o=100, ξ=0.05	5: h=10, R_o=100, ξ=0.05	↑	↓
3: h=8, R_o=120, ξ=0.05	7: h=10, R_o=120, ξ=0.05	↑	↓
2: h=8, R_o=100, ξ=0.10	6: h=10, R_o=100, ξ=0.10	↑	↓
4: h=8, R_o=120, ξ=0.10	8: h=10, R_o=120, ξ=0.10	↑	↓

Table 3.6. Comparisons of the model response in the form of $u(t) = U\sin(\omega t + \phi)$

Model	compared with Model	ξ	U
1: h=8, R_o=100, ξ=0.05	2: h=8, R_o=100, ξ=0.10	↑	↓
3: h=8, R_o=120, ξ=0.05	4: h=8, R_o=120, ξ=0.10	↑	↓
5: h=10, R_o=100, ξ=0.05	6: h=10, R_o=100, ξ=0.10	↑	↓
7: h=10, R_o=120, ξ=0.05	8: h=10, R_o=120, ξ=0.10	↑	↓

Table 3.7. Comparisons of the model response in the form of $u(t) = U\sin(\omega t + \phi)$

Model	compared with Model	R_o	U
1: h=8, R_o=100, ξ=0.05	3: h=8, R_o=120, ξ=0.05	↑	↓
2: h=8, R_o=100, ξ=0.10	4: h=8, R_o=120, ξ=0.10	↑	↓
5: h=10, R_o=100, ξ=0.05	7: h=10, R_o=120, ξ=0.05	↑	↓
6: h=10, R_o=100, ξ=0.10	8: h=10, R_o=120, ξ=0.10	↑	↓

From Table 3.5, it is clear that when depth of the beam h increases, time response function $u(t)$ decreases for a fixed time value.

It can be observed from Tables 3.6 and 3.7 that when damping ratio ξ and catenary parameter R_o increase, the magnitude U of the response function $u(t)$ is decreased.

CHAPTER 4

CONCLUSIONS

Time response of a planar curved beam with variable curvatures under in-plane impact load can be analyzed by two numerical methods which are Finite Difference and Finite Element Methods when the equation of motion with variable coefficients is not solvable exactly as in this study. The variable coefficients in the present equation of motion appear since the axis of the curved beam is function of the axial coordinate which is curvilinear coordinate system.

Mathematica for the solution with Finite Difference Method can be used to develop a computer program regarding the titled problem. For finite element models and solution ANSYS Parametric Design Language can be used effectively.

It is found that when catenary parameter R_o increases for all depth of the beam h in the range of considered in this study, first and fourth natural frequencies increase. However, the tendencies of natural frequencies observed for first and fourth natural frequencies reverse for second and third natural frequencies.

As related with the time response of the curved beam against to impact load, it is found that when depth of the beam h increases, time response function $u(t)$ decreases for a fixed time value. Also, when damping ratio ξ and catenary parameter R_o increase, the magnitude U of the response function $u(t)$ is decreased.

REFERENCES

Bhatti A.Q.,Kishi, N. 2011, An application of impact-response analysis on small-scale RC arch-type beams without stirrups. *Construction and Building Materials* 25: 3972–3976.

Cangar, F. 2013, In-plane free vibration analysis of laminated composite curved beams with variable curvature, M.Sc Thesis, Izmir Institute of Technology.

Clough, R.W. and Penzien, J. 2003. Dynamics of structures. Berkeley, Computers and Structures Inc.

Cook, R.D, Malkus, D.S., and Plesha, M.E. 1989, Concepts and applications of finite element analysis. New York: John Wiley and Sons, Inc.

Den Hartog, J.P., 1928. The lowest natural frequency of circular arcs. *Philosophical Magazine* 5: 400-408.

Gutierrez, R.H., Laura, P.A.A., Rossi, R.E., Bertero, R., Villaggi, A., 1989. In-plane vibrations of non-circular arcs of non-uniform cross-section. *Journal of Sound and Vibration* 129: 181-200.

Huang, C.S., Tseng, T.J., Leissa, A.W. 1996. An accurate solution for the in-plane transient response of a circular arch. *Journal of Sound and Vibration* 196: 595-609.

Huang, C.S., Tseng, Y.P., Leissa, A.W. and Nieh, K.Y. 1998a. An exact solution for in-plane vibrations of an arch having variable curvature and cross section. *International Journal of Mechanical Science* 40: 1159-1173.

Huang, C., Tseng, Y., and Lin, C. 1998b. ”In-Plane Transient Responses of Arch with Variable Curvature Using Dynamic Stiffness Method.” *Journal of Engineering Mechanics* 124: 826–835.

Inman, D.J., 2001. Engineering vibration. Upper Saddle River, New Jersey, Prentice-Hall.

Kohnke, P., 2004. ANSYS, Inc. Theory Reference. Canonsburg: ANSYS, Inc. online documentation or the ANSYS

Lee, B.K. and Wilson J.F. 1989. Free vibrations of arches with variable curvature. *Journal of Sound and Vibration* 136: 75-89.

Love, A.E.H. 1944. A treatise on the mathematical theory of elasticity. New York: Dover Publications.

Marur, S.R.; Kant, T. 2011. Transient dynamic analysis of higher order sandwich and composite arches *Computers & Structures* 93: 1201-1216.

Meirovitch, L. 2001. Fundamentals of vibrations. Singapore: McGraw-Hill Higher Education.

Oh, S.J., B.K. Lee, and I.W. Lee. 1999. Natural frequencies of non-circular arches with rotatory inertia and shear deformation. *Journal of Sound and Vibration* 219(1):23-33.

Oh, S.J., B.K. Lee, and I.W. Lee. 2000. Free vibrations of non-circular arches with non-uniform cross-section. *International Journal of Solids and Structures* 37:4871-4891.

Petyt, M. 2010. Introduction to finite element vibration analysis. Cambridge: Cambridge University Press.

Romanelli, E. and Laura, P.A. 1972. Fundamental frequencies of non-circular, elastic, hinged arcs. *Journal of Sound and Vibration* 24: 17-22.

Sakiyama, T. 1985. Free vibrations of arches with variable cross section and non-symmetrical axis. *Journal of Sound and Vibration* 102(3):448-452.

Sheinman, I. 1979, Forced vibration of a curved beam with viscous damping, *Computers and Structures* 10: 499-503.

Takahashi, S., Suzuki, K., Fukazawa, K., and Nakamachi, K. 1977. In plane vibrations of elliptic arc bar and sinus curve bar. *Bulletin of the Japan Society of Mechanical Engineers* 20: 1236-1243.

Volterra, E. and Morell, J. D. 1960. A note on the lowest natural frequency of elastic arcs, *Journal of Applied Mechanics* 27: 744-746.

Wang, T. 1972. Lowest natural frequency of clamped parabolic arcs. *Journal of Structural Division* 98:407-411.

Wang, T.M., Moore, J.A., 1973. Lowest natural extensional frequency of clamped elliptic arcs. *Journal of Sound and Vibration* 30: 1-7

White, A.R. 1954, Behavior of curved beams under impact loading, M.Sc Thesis, Georgia Institute of Technology.

Yardimoglu, B. 2010. Dönen eğri eksenli çubukların titreşim özelliklerinin sonlu elemanlar yöntemi ile belirlenmesi. 2. Ulusal Tasarım İmalat ve Analiz Kongresi, Balıkesir, 514-522

Yardimoglu, B. 2012. Lecture Notes on Mechanical Vibrations, Izmir: Izmir Institute of Technology.

Yıldırım, V. 1997. In-plane and out-of-plane free vibration analysis of Archimedes-type spiral springs. *Journal of Applied Mechanics* 64:557-561.

Yu, T.X., Symonds, P.S., and Johnson, W. 1985, A quadrantal circular beam subjected to radial impact in its own plane at its tip by a rigid mass, *Proc. R. Soc. Lond. A* :400, 19-36.

APPENDIX A

CENTRAL DIFFERENCES

Table A.1. Central differences approximations of O(h^2)

Term	Central Difference Expressions
$\frac{dw}{ds}$	$\frac{w(i+1)-w(i-1)}{2h}$
$\frac{d^2w}{ds^2}$	$\frac{w(i+1)-2w(i)+w(i-1)}{h^2}$
$\frac{d^3w}{ds^3}$	$\frac{w(i+2)-2w(i+1)+2w(i-1)-w(i-2)}{2h^3}$
$\frac{d^4w}{ds^4}$	$\frac{w(i+2)-4w(i+1)+6w(i)-4w(i-1)+w(i-2)}{h^4}$
$\frac{d^5w}{ds^5}$	$\frac{w(i+3)-4w(i+2)+5w(i+1)-5w(i-1)+4w(i-2)-w(i-3)}{h^5}$
$\frac{d^6w}{ds^6}$	$\frac{w(i+3)-6w(i+2)+15w(i+1)-20w(i)+15w(i-1)-6w(i-2)+w(i-3)}{h^6}$